The identification of airbursts in the past: Insights from the BIT-58 layer

Matthias van Ginneken, Ralph Harvey, Steven Goderis, Natalia Artemieva, Mark Boslough, Ryoga Maeda, Jérôme Gattacceca, Luigi Folco, Akira Yamaguchi, Penelope Wozniakiewicz, et al.

Earth Planet. Sci. Lett. 627 (2024) 118562

Contents lists available at ScienceDirect

Earth and Planetary Science Letters

journal homepage: www.elsevier.com/locate/epsl

The identification of airbursts in the past: Insights from the BIT-58 layer

Matthias van Ginneken [a,*], Ralph P. Harvey [b], Steven Goderis [c], Natalia Artemieva [d,e], Mark Boslough [f], Ryoga Maeda [g], Jérôme Gattacceca [h], Luigi Folco [i], Akira Yamaguchi [j], Corinne Sonzogni [h], Penelope Wozniakiewicz [a]

[a] Centre for Astrophysics and Planetary Science, School of Physical Sciences, University of Kent, Ingram Building, Canterbury CT2 7NH, UK
[b] Department of Geological Sciences, 112 A. W. Smith Building, Case Western Reserve University, Cleveland OH 44106-7216, USA
[c] Archaeology, Environmental Changes & Geo-Chemistry, Vrije Universiteit Brussel, Pleinlaan 2, Brussels BE1050, Belgium
[d] Planetary Science Institute, 1700 East Fort Lowell, Suite 106, Tucson AZ 85719, USA
[e] Russian Academy of Sciences, Institute of Geosphere Dynamics, Moscow 119334, Russian Federation
[f] Earth and Planetary Sciences, University of New Mexico, Albuquerque, NM 87131, USA
[g] Submarine Resources Research Center (SRRC), Japan Agency for Marine-Earth Science and Technology (JAMSTEC), 2-15 Natsushimacho, Yokosuka, Kanagawa 237-0061, Japan
[h] CNRS, Aix-Marseille Univ, IRD, INRAE, CEREGE, Aix-en-Provence, France
[i] Dipartimento di Scienze della Terra, Università di Pisa, Via S. Maria 53, Pisa, Italy
[j] National Institute of Polar Research, Tokyo 190-8518 Japan

ARTICLE INFO

Editor: Dr. F. Moynier

ABSTRACT

Airbursts are estimated to be the most frequent type ofdestructive impact events. Yet, confirmation of these events is elusive, resulting in a major gap in the impact record of Earth. The recent discovery of igneous chondritic spherules produced during a new type of touchdown airburst 430 thousand years (kyr) ago over Antarctica, in which a projectile vapor jet interacts with the Antarctic ice sheet, provided the first trace of such an impact in the geological record. In terms of petrology and geochemistry, particles constituting the BIT-58 dust horizon, which was found in surface ice at near Allan Hills in Antarctica, are almost identical to those produced 430 kyr ago. We demonstrate here that BIT-58 particles were indeed formed during a touchdown event between 2.3 and 2.7 million years (Myr) ago. This represents the oldest record of an airburst on Earth identified to date. Slight geochemical differences with 430 kyr old airburst spherules provide additional constraints on spherule condensation in large airburst plumes. Finding confirmation of airbursts in the paleorecord can provide insight into the frequency of the most hazardous impacts and, thus, has implications for planetary defence.

1. Introduction

Airbursts are the sharp release of impact energy when asteroids less than 200 m in size are disrupted in the lower atmosphere (Artemieva and Shuvalov, 2016; Boslough et al., 2015). Shockwaves and thermal radiation produced by airbursts result in massive damage at ground level, as evidenced by the 2013 Chelyabinsk small-scale airburst that resulted from the atmospheric entry of a stony asteroid approximately 20 metres in size (Popova et al., 2013). Surveys of the population of Near-Earth Asteroids smaller than 140 m, along with numerical models simulating effects at ground level, suggest that airbursts are currently the biggest cosmic threat to populations and infrastructures by combining their destructive potential and calculated frequency (Artemieva and Shuvalov, 2019; Boslough, 2014; Boslough et al., 2015). However, contrary to cratering events that can be identified using a set of well-defined geomorphological, mineralogical and geochemical criteria, evidence for past airbursts are poorly constrained (Glass and Simonson, 2012; Osinski et al., 2012). This is partly due to the lack of easily recognizable impact structures created by such events, but also a limited knowledge of physical and geochemical processes leading to the formation of potential residues.

The recent discovery of airburst spherules from Antarctica demonstrates that past airburst events can be identified on the grounds of petrological and geochemical evidences (Van Ginneken et al., 2021; 2010). So far, two spherule populations have been reported to have originated from large airbursts approximately 430 and 480 thousand

* Corresponding author.
E-mail address: m.van-ginneken@kent.ac.uk (M. van Ginneken).

https://doi.org/10.1016/j.epsl.2023.118562
Received 19 October 2023; Received in revised form 18 December 2023; Accepted 27 December 2023
Available online 9 January 2024

years ago over Antarctica. While both events were airbursts, their scale and regional effects were likely different. The older one was likely similar to the Tunguska event from 1908, where damage at ground level was mostly due to an intense shockwave and thermal radiations (Shuvalov and Artemieva, 2002). The younger event was described as a touchdown event, or type II airburst, when the jet of vaporized impactor material does not lose momentum and reaches ground level at hypervelocity, resulting in chemical exchange between projectile superheated gas and vaporized ground material, in this case Antarctic ice (Boslough and Crawford, 2008; Van Ginneken et al., 2021). These two airburst spherule populations suggest that airburst events may have varied extensively in scale in the past, from normal airbursts not reaching ground level to relatively large touchdown events.

The airburst spherules discovered so far are igneous and holocrystalline, exhibiting petrological and textural properties reminiscent of cosmic spherules, that is melted micrometeorites, and microkrystites (Genge et al., 2008; Glass and Burns, 1988; Margolis et al., 1991). However, subtle morphological and geochemical differences, when combined, appear to strongly point to a formation during airbursts, such as a spherulitic structure that suggests coalescence of spherules in a dense, hot and turbulent cloud; different types of spherules exhibiting varied petrogenesis indicating mixing in a complex and dynamically evolving plume; an absence of aerodynamical features (e.g., tails) consistent with condensation instead of melting of meteoritic material; volatile-bearing bulk composition due to formation in a dense plume preventing their efficient degassing; iron spinel compositions indicating a wide range of oxygen fugacity consistent with complex formation pathways in a heterogeneous and turbulent plume. In the case of the 430 kyr old event, interaction of the jet of superheated meteoritic gas with the Antarctic ice sheet was suggested on the basis of ^{18}O-depleted oxygen isotopic signatures consistent with mixing of projectile gas with Antarctic ice vapor. Finding additional populations of airburst spherules is critical to define them as a robust tool to identify airbursts in the geological past.

In 1994, the unusual BIT-58 extraterrestrial dust horizon was found during the systematic sampling of blue ice tephra (BIT) layers cropping out near the Allan Hills blue ice field, Antarctica (Fig. 1a; (Harvey et al., 1998). The broadly chondritic composition of 95 % of the particles constituting this dust horizon attests for an extraterrestrial origin, whereas the remining 5 % are tephra and detritus from local rocks. The extraterrestrial particles exhibit an olivine-rich holocrystalline lithology, with more than 40 % of them being spheroidal (Figs. 2 and S1). On the basis of their petrology and chemistry, Harvey et al. (1998) suggested that BIT-58 particles were deposited during a single event by the ablation of a large H-chondrite over Antarctica. The age of the event was estimated at 2.3 to 2.7 Myrs on the basis of cosmogenic nuclide concentrations (Harvey et al., 1998). Interestingly, BIT-58 particles exhibit a range of structural and petrological properties consistent with ca. 430 kyr old airburst spherules (Van Ginneken et al., 2021). Here we explore BIT-58 particles further, using the methodology developed by (Van Ginneken et al., 2021). We demonstrate that these particles represent a third distinct airburst spherule population in Antarctica, which has implications for the identification of such hazardous events in the geological record.

2. Materials and methods

2.1. Sample extraction

The BIT 58 was discovered during the systematic sampling of tephra layers near Allan Hills in 1994 (Fig. 1). The presence of a high proportion of dark spheroidal particles distinguished this layer from the volcanic glass and phenocrysts typically present in tephra layers, prompting the extraction in early 1995 of roughly 100 kg of ice that included BIT 58. The blocks of ice were then transported to the Crary Lab at McMurdo Station, Antarctica, where they were cleaned with de-ionized water,

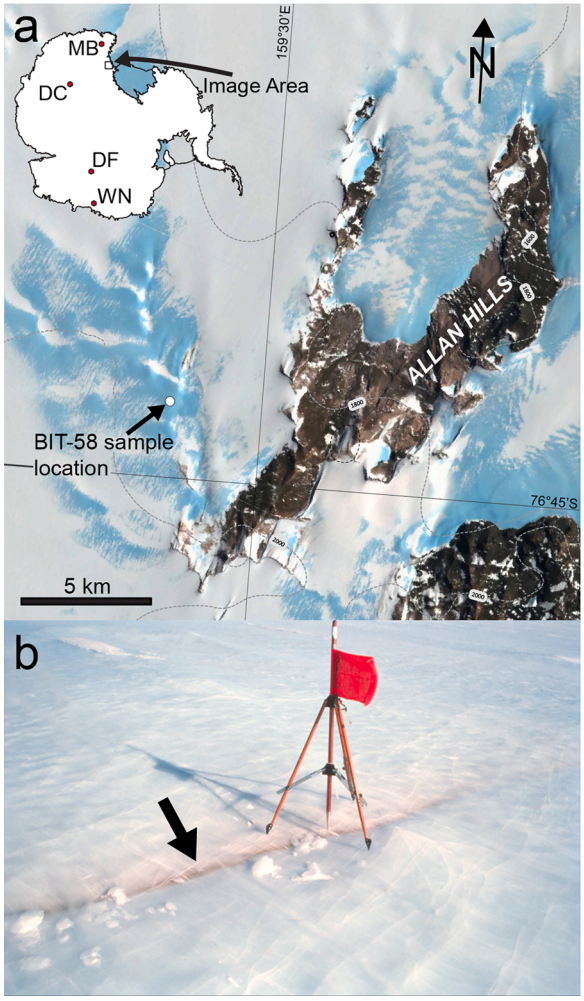

Fig. 1. Location of the BIT-58 sampling site. a) Landsat image of the sampling site at BIT-58 near Allan Hills, Victoria Land, Antarctica. Inset shows the locations of Dome Fuji (DF), Dome Concordia (DC), Miller Butte (MB) and Walnumfjellet (WN) for comparison (Misawa et al., 2010; Narcisi et al., 2007; Van Ginneken et al., 2021, 2010). b) The BIT-58 debris layer as it appeared before sampling of surface ice. The satellite map was made using the Quantarctica mapping environment for QGIS (Matsuoka et al., 2021). Photo credit: Ralph P. Harvey, Case Western Reserve University.

melted in a microwave, and sieved using 64 and 3 μm meshes . Subsequently, obvious terrestrial particles were removed manually under a stereo microscope. The discovery and sample extraction are available in Harvey et al. (1998). For this study, 116 extraterrestrial particles from the BIT-58 sample were randomly selected, embedded in Epoxy resin and subsequently sectioned and polished using polishing paper and aluminum paste.

2.2. Major element chemistry

Major and minor elemental compositions were determined using a JEOL JXA-8200 electron probe micro analyzer (EPMA) at the National Institute of Polar Research (Tokyo, Japan) on the embedded and polished BIT-58 particles. All analyses were carried out using a 15 kV accelerating voltage. Their sulfide phases were analyzed using a focused beam with a diameter of less than 1 μm at 30 nA beam current while monitoring the elements Mg, Al, Si, P, S, Cr, Fe, Co, Ni, Cu, and Zn. Silicate and oxide phases were analyzed using a focused beam with a diameter of less than 1 μm at 10 nA beam current while monitoring Na, Mg, Al, Si, P, S, Cl, K, Ca, Ti, V, Cr, Mn, Fe, Co, and Ni. A beam diameter

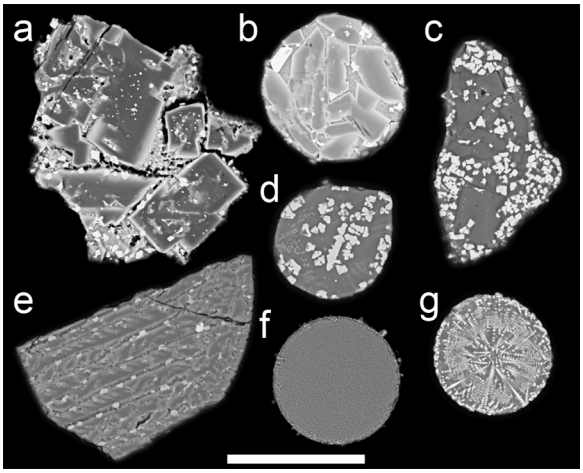

Fig. 2. Representative scanning electron backscattered images of sectioned BIT-58 particle types. (a) A Spinel-Poor Angular (SPA) particle, which consists in euhedral olivine, minor cosmic spinel (< 10 vol.%), minor interstitial glass and metal inclusions in olivine. (b) A Spinel-Poor Spherical (SPS) spherule, which shares properties with SPA particles expect in the spherical shape. (c) A Spinel-Rich Angular (SRA) particle, which consists in subhedral or skeletal olivine, with abundant cosmic spinel (>20 vol.%) and minor interstitial glass. (d) A Spinel-Rich Spherical (SRS) spherule, which is similar to SRA particles except in its spherical shape. (e) Fragment of a barred olivine (BO) spherule that exhibit a barred olivine texture with minor cosmic spinel and interstitial glass. (f) A cryptocrystalline (CC) spherule consisting of submicrometric olivine and spinel in glass. (g) A dendritic spinel (DS) particle made of dendrites of spinel in glass with minor olivine. Scale bar is 50 μm.

of 20 μm was also used with the same condition as the silicate and oxide phases for "bulk" analysis. Counting times ranged from 10 to 100 s on peaks for each mineral. Correction procedures are based on the ZAF method. As a result of the occurrence of overlapping signals, the intensities of V, Co, and Cu were mathematically corrected for the intensities of Ti, Fe, and Ni, respectively. Natural and synthetic silicates, oxides, and metals with well-known chemical compositions were used as standards.

2.3. Oxygen isotope analyses

We measured the oxygen isotopic compositions of BIT-58 particles with a CAMECA IMS 1270 E7 at the center de Recherches Pétrographiques et Géochimiques (Nancy, France). $^{16}O-$, $^{17}O-$, and $^{18}O-$ ions produced by a Cs^+ primary ion beam (~10 μm and ~2 nA) were detected in multicollection mode using two off-axis Faraday cups (FCs) for $^{16}O-$ and $^{18}O-$ and the axial FC for $^{17}O-$. To remove the $^{16}OH-$ interference on the $^{17}O-$ peak and to obtain maximum flatness on the top of the $^{16}O-$ and $^{18}O-$ peaks, entrance and exit slits were adjusted to acquire a mass resolving power (MRP) of ≈7000 for $^{17}O-$ on the central FC. The multicollection FCs were set on slit 1 (MRP = 2500). The total measurement time was 270 s (180-s measurement + 90-s presputtering). We used four in-house terrestrial standard materials (San Carlos olivine, CLDR01 MORB glass, Charroy magnetite, and JV1 diopside) to (i) define the instrumental mass fractionation line for the three oxygen isotopes and (ii) to correct the instrumental mass fractionation due to the matrix effect in samples. Typical count rates obtained on the San Carlos olivine standard were 1×10^9 cps for ^{16}O, 3.5×10^5 cps for ^{17}O, and 1.8×10^6 cps for ^{18}O. The 2σ errors were ≈0.4‰ for $\delta^{18}O$, ≈0.7‰ for $\delta^{17}O$, and ≈0.8‰ for $\Delta^{17}O$ ($\Delta^{17}O$ representing the deviation from the TFL, $\Delta^{17}O = \delta^{17}O - 0.52 \times \delta^{18}O$).

3. Results

The particles are black, exhibiting a wide range of morphologies, the majority being angular or sub-angular and about 30 % (N = 36) being perfectly spherical. Scanning electron microscopy (SEM) shows that about 10 % (N = 13) of the particles are compound spherules consisting of several coalesced spherules (Fig. 3). Polished sections of the particles show quench textures similar to the 430 kyr old airburst spherules from Walnumfjellet nunatak (hereafter WN), including porphyritic olivine, barred olivine, dendritic iron spinel and cryptocrystalline (Fig. 2; Van Ginneken et al., 2021). The mineralogy of the particles mainly consists of olivine, iron spinel and minor interstitial glass, with accessory sulfide inclusions in the larger euhedral olivine crystals. Particles were then subdivided into seven groups on the basis of their shape, textures and spinel content: (i) Spinel-Poor Angular (SPA) particles (N = 54) characterized by angular shapes and large (>10 μm) skeletal or euhedral crystals of olivine with minor cubic spinel content (<10 % volume) (Figs. 2a and S1a); (ii) Spinel-Poor Spherical (SPS) particles (N = 13) that differ from SPA only in their spherical shape (Figs. 2b and S1b); (iii) Spinel-Rich Angular (SRA) particles (N = 17) characterized by their sub-angular shape, abundant octahedral, cruciform and/or dendritic spinel (≥18 % volume), and skeletal and/or euhedral olivine (Figs. 2c and S1c); (iv) Spinel-Rich Spherical (SRS) particles (N = 14) which differ from particles SRA only in their spherical shapes (Figs. 2d and S1d); (v) barred olivine (BO) particles (N = 7) that contain minor spinel content (<10 % volume; Figs. 2e and S1e); (vi) cryptocrystalline (CC) particles exhibiting submicron olivine crystals and moderate spinel content (Figs. 2f and S1f); and (vii) dendritic spinel (DS) particles exhibiting spinel dendrites and minor olivine in glass (Figs. 2g and S1g). The size of the particles were estimated from the SEM images and we assumed that the irregularly shaped particles are ellipsoids with equal minor and intermediate axes (a ≥ b = c). To calculate their representative size we used $3\sqrt{(a * b^2)}$. Regardless of groups size ranges from about 30 to 120 μm. Size does not vary significantly from one group to the other: 71 ± 18 (1σ) μm for SPA particles, 75 ± 12 μm for SPS particles, 75 ± 12 μm for SRA particle, 60 ± 11 μm from SRS particles, 75 ± 12 μm for BO particles, 60 ± 12 μm for CC particles, and 85 ± 13 μm for DS particles.

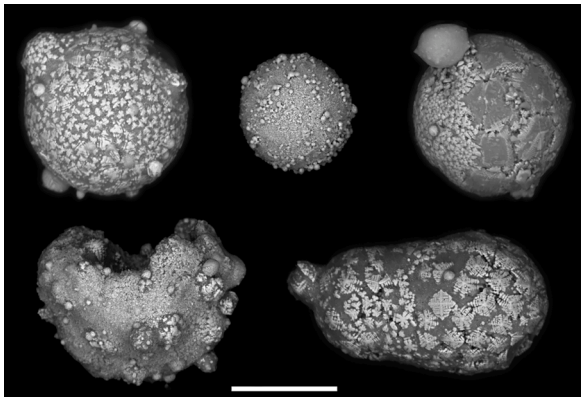

Fig. 3. Scanning electron backscattered images of BIT-58 compound spherules showing evidence of coalescence of several spherules. Scalebar is 50 μm.

Electron microprobe defocused beam analyses of major and minor elements in BIT-58 particles are reported in table S1 and displayed in Fig. S2, while averaged bulk compositions of each types described above are shown normalized to CI chondrites in Fig. S3. Similarly to what was reported by Harvey et al. (1998), elemental patterns show consistent chondritic compositions, albeit with slight enrichment and depletion in alkali elements in SRA/SRS and SPA/SPS particles, respectively, notable depletion in Cr in SRS and DS particles, and severe depletion in S in all particles, albeit to a lower extent in SPA/SRS particles. Major and minor element composition of individual phases was determined using a focused electron beam. The composition of olivine is reported in table S2. The SRS particles are predominately Fe-poor ($Fa_{7\pm2}$), whereas other particle types are relatively Fe-rich ($Fa_{23\pm5}$). Olivine is consistently nickel-rich, with an average NiO content of 2.00 ± 0.57 wt%. The major

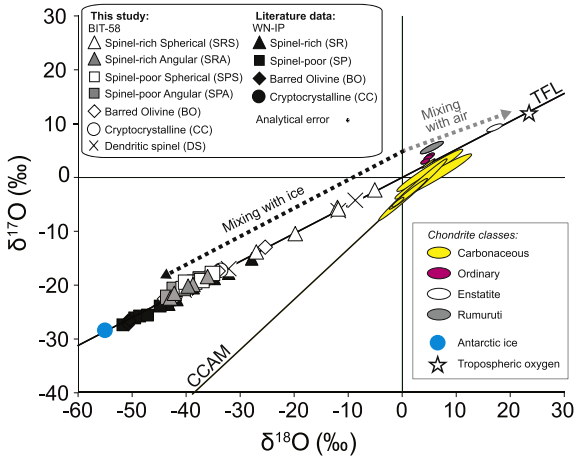

Fig. 4. $\delta^{17}O$ versus $\delta^{18}O$ diagram (values in ‰ versus V-SMOW) for BIT-58 particles, compared to WN particles (Van Ginneken et al., 2021). Antarctic inland ice values from (Kawamura et al., 2017) and tropospheric oxygen values from (Thiemens et al., 1995). Bulk isotopic compositions of chondritic meteorites are represented in rounded colored shaded areas, including carbonaceous chondrites [i.e., below the terrestrial fractionation line (TFL)], ordinary and Rumuruti chondrites (i.e., above the TFL), and enstatite chondrites (i.e., on the TFL) ((Clayton et al., 1991; Clayton and Mayeda, 1999; Newton et al., 2000)). The dashed lines illustrate the effects of oxygen isotopic exchange of a chondritic impactor with Antarctic ice and atmospheric air.

and minor composition of individual iron spinel grains in SPA, SPS, SRA and SRS particles is reported in table S3. In SRS and SRA particles, spinel exhibits high-Mg and high-Ni concentrations on average (MgO = 12.36 ± 0.64 and 6.08 ± 1.62 wt%, NiO = 4.39 ± 0.51 and 2.96 ± 0.88 wt%, respectively), indicating important magnesioferrite and trevorite components, and minor magnetite. Conversely, spinel crystals exhibit lower Mg and Ni concentrations in SPS and SPA particles (MgO = 1.68 ± 0.79 and 1.09 ± 0.73 wt%, NiO = 0.52 ± 0.09 and 0.33 ± 0.21 wt%, respectively). The oxygen isotopic compositions of the particles was determined using secondary ion mass spectrometry (SIMS) and exhibit systematically negative $\delta^{18}O$ values (Fig. 4 and Table S4). The δ18O values in types SPA, SPS, BO and CC overlap and range from −43.8 to −25.2‰, whereas type SRS exhibit notably higher values ranging from −26.8 to −4.8‰. Types DS exhibit the widest range from −40.2 to −8.4‰. The $\Delta^{17}O$ values, which illustrates the spread from the terrestrial fractionation line (TFL), are positive (N = 26) and negative (N = 8) and range from −0.49 to 0.90‰.

4. Discussion

4.1. Formation of BIT-58 particles in a dense and turbulent touchdown airburst plume

As already demonstrated by Harvey et al. (1998), the chondritic composition of BIT-58 particles clearly points to an extraterrestrial origin. Their quenched textures and simple mineralogy are reminiscent of S-type and G-type cosmic spherules, which are silicate and dendritic magnetite rich melted micrometeorites respectively (Folco and Cordier, 2015; Genge et al., 2008). However, obvious differences include the high bulk nickel and alkali content, and high magnesioferrite component in iron spinel. The precursors of cosmic spherules melt at an altitude of 70 to 90 km, where the tenuous atmosphere and low oxygen partial pressure result in the near total degassing of volatiles (typically Na and K) and limited oxidation of metallic (Fe^0) and ferrous (Fe^{2+}) iron result in the formation of magnetite ($Fe^{2+}Fe_2^{3+}O_4$), respectively (Folco and Cordier, 2015; Toppani and Libourel, 2003). Therefore, BIT-58 are clearly incompatible with the more volatilized and less oxidized cosmic spherules. Furthermore, BIT-58 form a discrete layer of dark dust visible on the exposed blue ice, parallel to tephra layers, suggesting concentrations well in excess of the background cosmic dust flux (Fig. 1b). Together with the narrow range of chemical composition exhibited by BIT-58 particles, regardless of the type, this suggests that the particles were deposited during a single meteoritic event, in accordance with observations reported by Harvey et al. (1998).

Other microscopic igneous impact spherules discovered so far include spherules produced during cratering events and large airbursts (Glass and Simonson, 2012; Van Ginneken et al., 2021, 2010). Microtektites and microkrystites are produced when a large asteroids impacts ground material and mainly consist of target material. Microtektites are typically melt products consisting mostly of crustal material giving their generally acid composition, with trace amounts of impactor; their often clear and glassy aspect reflects an absence of crystallites (Glass and Simonson, 2012). Furthermore, aerodynamic shapes are frequently observed in populations of microtektites, such as dumbbell or teardrop morphology, pointing to their deposition after travelling along ballistic trajectories (Folco et al., 2008). Based on these criteria alone, BIT-58 particles can be distinguished with confidence from microtektites. Microkrystites on the other hand are characterized by their translucent pale to dark aspect reflective of their high crystallinity (Glass and Simonson, 2012). Their basic composition is due to a larger impactor component compared to microtektites and they are thought to form by condensation in the impact plume, thanks to their spherical shapes (Glass and Burns, 1988). In this regards, BIT-58 are similar to microkrystites. However, the texture of microkrystites are typically dendritic with a large glass component, which is in clear contrast to most BIT-58 particles, which exhibit porphyritic textures (i.e. SPA, SPS, SRA and SRS types). A unique type of impact spherule are those associated with the Eltanin impact, which is thought to have occurred about 2.15 Myrs ago in the Bellingshausen Sea, off the coast of Antarctica (Margolis et al., 1991). These mafic spherules are thought to be mainly constituted of a meteoritic component, as opposed to microtektites and microkrystites, and to have been deposited in seawater close to the crater (Gersonde et al., 1997). Compound spherules are frequently observed, suggesting coalescence in the impact plume, as well are aerodynamically shaped spherules inconsistent with BIT-58 particles. Furthermore, the Eltanin impactor is thought to have been an achondritic asteroid (i.e., a low-metal mesosiderite; (Kyte, 2002), which is inconsistent with BIT-58. Overall, BIT-58 particles do not bear striking resemblance to known spherules resulting from impact cratering events.

Conversely, BIT-58 particles are almost identical to airburst spherules from Walnumfjellet nunatak (WN), especially in terms of textural variability (Van Ginneken et al., 2021). Indeed, spinel-poor (SP) and spinel-rich (SR) particles, as well as barred olivine and cryptocrystalline

Table 1
Major element composition of BIT-58 particles compared to airburst spherules from Walnufjellet Nunatak (WN) and the Transantarctic Mountains (TAM).

	BIT-58	WN[a]	TAM[b]
Na2O	1.07 ± 0.46	0.83 ± 0.60	1.29
Al2O3	2.42 ± 0.50	2.48 ± 1.29	2.49
K2O	0.10 ± 0.04	0.06 ± 0.05	0.10
TiO2	0.10 ± 0.03	0.09 ± 0.05	0.12
FeO	31.6 ± 4.9	31.8 ± 6.6	28.9
MgO	24.4 ± 3.5	25.5 ± 7.4	24.3
SiO2	35.9 ± 3.3	34.9 ± 2.6	35.5
CaO	2.03 ± 0.45	1.97 ± 1.08	2.02
Cr2O3	0.43 ± 0.19	0.42 ± 0.18	0.60
MnO	0.37 ± 0.06	0.38 ± 0.05	0.29
S	0.44 ± 0.28	0.02 ± 0.05	0.14
P2O5	0.37 ± 0.12	0.29 ± 0.15	0.24
NiO	1.50 ± 0.56	1.79 ± 0.54	1.69
CoO	0.11 ± 0.04	ND	ND

[a] data from Van Ginneken et al. (2021).
[b] data from Van Ginneken et al. (2010)
ND = not determined.

spherules from WN are almost indistinguishable from the SPA/SPS, SRA/SRS, BO and CC spherules described above (Figs. 2 and S1). A similar observation can be made for the 480 kyr old airburst spherules discovered at Miller Butte in the Transantarctic Mountains (TAM) that show the same variations in textures among particles (Van Ginneken et al., 2010). Furthermore, the average chondritic bulk compositions of BIT-58 particles match those of spherules from WN and TAM (Table 1). More interestingly, the $\delta^{18}O$ values of BIT-58 particles is systematically negative like those of WN spherules (Fig. 4). Van Ginneken et al. (2021) noted that such negative $\delta^{18}O$ values point to interaction with Antarctic ice during contact of the airburst plume with the icesheet and shortly before formation of the WN airburst spherules. Indeed, there is a lack of other reservoirs having negative $\delta^{18}O$ which, upon mixing with chondritic material having $\delta^{18}O$ plotting near 0‰, may have resulting in values observed in WN (and, thus, BIT-58) spherules. Contamination by ice of BIT-58 particles during storage for over 2 Myrs by terrestrial weathering can be ruled out as none of the particles exhibit alteration features, such a dissolution or topotactic replacement of primary mineral phases, which are typical in igneous extraterrestrial spherules from TAM including airburst spherules (van Ginneken et al., 2016; Van Ginneken et al., 2010).

Airbursts are typically assumed to result in destructive shockwaves and thermal radiation that are the main factors leading to damage at ground level (Artemieva and Shuvalov, 2016). However, hydrocode airburst simulations have shown that in the case of stony asteroids approximately 150 m in diameter, the jet of superheated gas produced by the vaporization of the asteroid will not lose momentum before reaching ground level at hypervelocity (Van Ginneken et al., 2021). To describe this unusually large airburst scenario, these authors coined the term 'touchdown scenario'. Another argument pointing towards such a scenario is the unusual composition of iron spinel in WN spherules, which is an excellent recorder of oxygen fugacity of the environment of formation of the spherules (Gayraud et al., 1996; Robin et al., 1992). Iron spinel synthesis experiments have shown that increasing oxidizing conditions result in Mg^{2+} and Ni^{2+} replacing Fe^{2+}, and Fe^{3+} replacing Al^{3+} and Cr^{3+}. Figure S4 shows the compositional trends of iron spinel in BIT-58 SPA, SPS, SRA and SRS particles, compared to spinel in WN SP and SR spherules as well as in TAM spherules. Similar compositional trends are observed with BIT-58 and WN spinels, although it is notable that BIT-58 systematically exhibit more extreme compositions at the lower and higher end of the trends, whereas TAM spinel compositions overlap spinel compositions in types SRA, SRS and SR. The Fe^{3+}/Fe_{tot} of iron spinel can also be used as a proxy to oxygen fugacity (Gayraud et al., 1996). Fig. 5 show the Fe^{3+}/Fe_{tot} in the various types of BIT-58 and WN spherules, as well as in TAM airburst spherules, K-Pg impact spherules, meteorite fusion crusts and micrometeorites (Ebel and Grossman, 2005; Gayraud et al., 1996; Genge and Grady, 1999; Robin et al., 1992; Van Ginneken et al., 2021, 2010). It is immediately apparent that the trend exhibited by iron spinel in BIT-58 SPA/SPS and SRA/SRS particles matches that of iron spinel is WN SP and SR airburst spherules, although SPA/SPS particles show the lowest Fe^{3+}/Fe_{tot} ratios of all particles listed. Iron spinel in TAM airburst spherules and the fusion crusts of meteorites overlap with BIT-58 SRA/SPS and WN SR particles. Similarly, iron spinel K-Pg impact spherules show a similar overlap, although they uniquely go to Fe^{3+}/Fe_{tot} near 100 %. Finally, iron spinel in micrometeorites plots at the lower end of the BIT SRA/SRS and WN SR particles. The spinel compositional trend of WN airburst spherules was interpreted as the result of different locations of condensation of pure chondritic gas within an airburst plume having heterogeneous oxidizing conditions. Indeed, WN SR spherules likely formed in a location of the plume where oxygen fugacity was relatively high, typically the periphery where turbulent mixing with atmospheric oxygen is likely, resulting in high spinel content and higher Fe^{3+}/Fe_{tot} values. Conversely, WN SP spherules formed in an area of the plume where conditions were much less oxidizing, most likely the center of the plume where the intrinsic oxygen fugacity of chondritic material and no injection of atmospheric oxygen resulted in very low spinel content and Fe^{3+}/Fe_{tot} values even lower than in micrometeorites (Brett and Sato, 1984). The injection of vaporized Antarctic ice and potential dissociation of water during formation of the WN spherules probably had a minimal effect on oxygen fugacity (Van Ginneken et al., 2021). Indeed, at low temperatures, the oxidizing potential of high-temperature water vapor is moderated by the production of H_2 and 2H; after sequestration of large amounts of free by, for example, condensation of silicate droplets, the remaining hydrogen is likely to cause reduction. This is also consistent with the textures and oxygen isotopic compositions of WN SP and SR spherules. Indeed, SP spherules exhibit large phenocrysts of euhedral olivine consistent with relatively slow cooling rates, whereas SR spherules show systematically smaller grain-size suggesting high cooling rates. Oxygen isotopic exchange also increase from WN SR to SP particles, which was interpreted as the former having $\delta^{18}O$ pulled towards positive atmospheric values whereas the latter formed in the core of the plume where near exchange with Antarctic ice occurred.

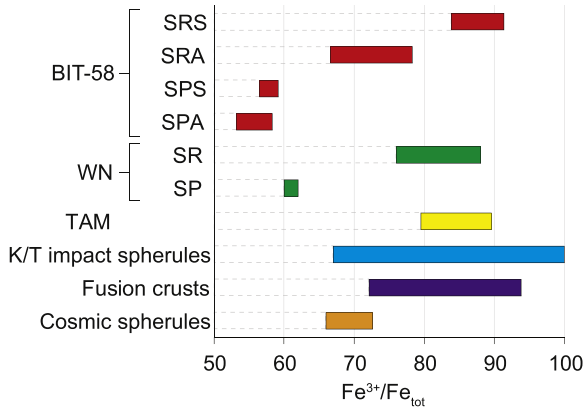

Fig. 5. Ranges of Fe^{+3}/Fe_{tot} ratios in cosmic spinel of BIT-58 particles, WN particles, TAM particles, K-Pg impact spherules (Ebel and Grossman, 2005; Gayraud et al., 1996; Robin et al., 1992; Van Ginneken et al., 2021, 2010).

We have shown that BIT-58 particles are nearly identical to WN airburst spherules in their textures, bulk composition, unusual oxygen isotopic signatures and, finally, unique iron spinel composition trends. Considering the uniqueness of these two populations of particles, it seems reasonable to assume that BIT-58 particles represent evidence for a touchdown event that occurred over the Antarctic icesheet between 2.3 and 2.7 Myrs ago.

While BIT-58 and WN were likely produced by similar processes, notable differences between the two particle populations exist. All descriptions below pertaining to WN spherules are from (Van Ginneken et al., 2021). In terms of size, WN spherules are typically >200 μm, whereas BIT-58 particles are <120 μm. Furthermore, while the bulk compositions are similar, BIT-58 are significantly richer in sulfur, which is evidenced by the presence of Fe-Ni-S metal inclusions in the interstitial glass of SPA, SPS and even CC particles (Fig. 2a and Table S5). Metal blebs a few micrometres in size are also observed in euhedral olivine crystals of SPA and SPS particles, although due to their small size their chemistry could not be analysed with confidence. Such inclusions and metal blebs are absent in WN SP airburst spherules. Furthermore, while the iron spinel compositional trends are similar, BIT-58 exhibit systematically more extreme Fe^{3+}/Fe_{tot} values, below 60 at% or above 90 at%, whereas WN spinel plot well within these two values (Figs., 5 and S4). Similarly, while $\delta^{18}O$ values in both populations are negative, WN spherules are mostly concentrated between ~−50 and −40‰ with a maximum value of −32‰, whereas BIT-58 particles are concentrated between ~−45 and −30‰ with a maximum value of −8‰ (Fig. 4). Furthermore, the BIT-58 SPA, SRA and DS types are not observed among WN spherules. It is noteworthy that while the presence of fine features on compound spherules suggest that some particles were not

damaged by movement of ice, the sharp aspect of SPA and most BO particles and frequent broken olivine crystals suggest that damage during storage in ice occurred. It is likely the initial particles were larger and, possibly, had a more rounded aspect. The difference between BIT-58 and WN particles listed above point to formation from two distinct airburst events. This makes sense considering the incompatible ages of both touchdown events, with BIT-58 estimated to be over 2 Myr old, whereas WN particles occurred approximately 403 kyr ago (Harvey et al., 1998; Van Ginneken et al., 2021). Thus, BIT-58 particles point to the identification of a third airburst event over Antarctica.

The discrepancy in oxygen isotope ranges between BIT-58 and WN particles can be explained by the isotopic composition of Antarctic ice, which can vary significantly through time. For instance, ice analyses from the EPICA Dome C ice core and surface ice near the Sør Rondane Mountains have shown a wide variation in $\delta^{18}O$ from −60 to −44‰ over the last 800kyrs (Grisart et al., 2022; Zekollari et al., 2019). The fact that for both populations most isotopic values plot in a narrow range is consistent with extensive mixing of the plume with ice vapor during particle formation. Therefore, we estimate that surface ice associated with the BIT-58 event had a much higher $\delta^{18}O$ value, possibly between −50 and −45‰, than the ice associated with the WN event, which was likely −55‰ (Kawamura et al., 2017).

With regards to the formation process of BIT-58 particles, it was likely similar to that of WN particles, that is condensation in a dense and turbulent plume shortly after contact with the Antarctic icesheet. As such, the numerical simulation of a touchdown impact resulting from a stony asteroid 150 m in size presented in Van Ginneken et al. (2021) is still applicable. Fig. 6a shows a snapshot of this numerical model at 10 s after contact with the ice sheet. While the temperature is still in excess of 5000 K in the core of the plume, it rapidly drops to temperatures consistent with condensation of silicate melts. Thus, this snapshot represents the structure of the airburst plume shorty before particle condensation, regardless of temperature. Fig. 6b shows a simplified illustration of an airburst plume when the different types of BIT-58 start condensing. The iron spinel composition and large grain size of SPA and SPS particles suggest that these formed in the least oxidizing and hottest part of the plume, that is near the core, where mixing with atmospheric oxygen is minimal and cooling rates are lowest (Figs. 2a, b, 5 and S4). Intense mixing with ice vapor explain why these particles exhibit the lowest $\delta^{18}O$ near Antarctic ice values (Fig. 4). The difference between these two types is mainly morphological and does not seem to be principally related to their formation processes. Based on their $\delta^{18}O$ values, it is likely CC particles formed in this region of the plume as well, before being quickly ejected to lower temperature regions where the cooling rates were higher, explaining the almost glassy texture. The iron spinel abundance and composition of SRA particles suggest that these formed in a more oxidizing region of the plume compared to SPA/SPS particles, whereas oxygen isotopes imply intense mixing with ice vapor (Figs. 2c, 4, 5 and S4). Their sub-angular shapes, as well as evidence for coalescence with smaller spherules (Fig. 3), suggest that these formed in the region of the plume where particle density, and thus interaction, was highest. We suggest that these particles first condensed near the core of the plume, where mixing with ice vapor is highest, before rapid turbulent motion during plume evolution sent them towards the oxygen-rich periphery. SRS particles show a high degree of oxidation, consistent with iron spinel forming in the troposphere, and exhibit $\delta^{18}O$ furthest from ice values and closest to atmospheric oxygen (Figs. 4, 5 and S4). Furthermore, their grain-size suggest relatively high cooling rates (Fig. 2d), pointing to a formation on the periphery of the plume where turbulent mixing with atmospheric oxygen was highest. The oxidation degree of BO and DS could not be determined due to the limited size of spinel crystals, however, their oxygen signatures suggest that the former may have formed in a region rich in ice vapor, whereas the latter may have formed in both the core and periphery of the plume. The propagation of the airburst plume along the rarefied wake left by the passage of the asteroid occurs in a matter of minutes after the impact; this results in efficient mixing and injection of the various particle types into the upper troposphere, before gravitational collapse of the cloud and settling of particles over larger distance (Artemieva and Shuvalov, 2016). Overall, BIT-58 particles show a formation process similar to WN airburst spherules (Van Ginneken et al., 2021).

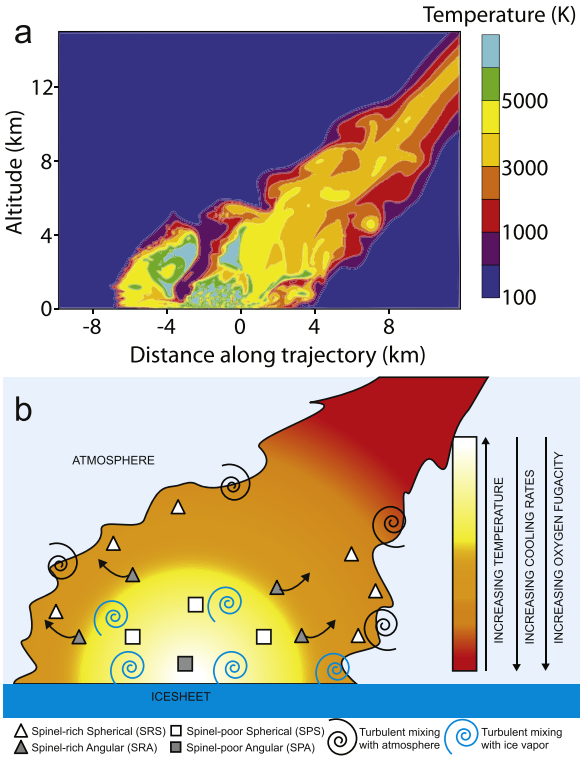

Fig. 6. (a) Temperature distribution in the impact plume 10 s after the contact with the ice sheet. Information on the numerical model used here is available in (Van Ginneken et al., 2021). (b) A simplified version of the simulation in (a) showing the location of formation of the various types of BIT-58 particles: SPA/SPS particles condense near the core of the plume, where cooling rates are slowest and oxygen fugacity lowest; SRA particles condense between near the innermost part of the plume before migrating to the oxygen-rich periphery; finally, SRS particles condense on the periphery of the plume, where cooling rates are fast and turbulent mixing with atmospheric oxygen is most efficient.

Determining the nature of an impactor responsible for airbursts in not trivial. In the past, impactors responsible for the TAM and WN airburst spherules have been estimated to be carbonaceous asteroids based on the oxygen isotope compositions of the spherules (Van Ginneken et al., 2021, 2012). However, the oxygen isotope values of BIT-58 particles seem less discriminative of a particular chondritic material . Most BIT-58 particles plot above the TFL, however isotopic trends between various particle types point both above and below this line, making the identification of the impactor difficult (Fig. 4). Using the bulk composition of BIT-58 particles and comparing to chondritic materials, Harvey et al. (1998) suggested that their progenitor was a H chondrite. Such an hypothesis is consistent with the presence of metal/sulfide inclusions in SPA/SPS spherules and their lowest Fe^{3+}/Fe_{tot}, suggestive of relatively reducing conditions in the airburst plume in which the particles condensed. Indeed, H chondrites are among the most reduced chondritic materials, as evidenced by the higher abundance of metallic iron and sulphides, as well as direct measurement of their intrinsic oxygen fugacity below the Iron-Wüstite buffer, compared to the more oxidized carbonaceous chondrites (Brett and Sato, 1984; Rubin et al., 1988). While more data is needed, such as Cr and Ti isotopic signatures, identifying the BIT-58 impactor as a H chondrite, or at the very least ordinary chondrite, appears credible. Finally, the continental distribution of spherules produced by the 430 and 480 kyrs airbursts was

established because of their occurrences in geographically distinct sites (Misawa et al., 2010; Narcisi et al., 2007; Van Ginneken et al., 2021, 2010). Geographical distribution as well as particle density allowed the determination of an impactor mass on the order of 10^9 kg and 10^8 kg for the 430 kyr and 480 kyr old events, respectively, which is consistent with airburst forming asteroids (Artemieva and Shuvalov, 2019). Such an estimation for the event recorded at BIT-58 is not possible as the geographical distribution is unknown.

4.2. Implications for the identification of airburst events in the geological record

The BIT-58 particles point to a third airburst event that occurred over Antarctica in the past, along with the 430 and 480 kyrs old events, as well as the second touchdown event (Van Ginneken et al., 2021, 2010). Particles produced during these airbursts share petrological and geochemical characteristics not usually combined in other igneous extraterrestrial spherules, from cosmic to impact spherules (Folco and Cordier, 2015; Genge et al., 2008; Glass and Simonson, 2012). This include the occurrence of compound spherules as evidence of coalescence in a dense and turbulent plume, which are not observed among cosmic spherules and rare in meteoritic ablation spheres due to microscopic size in space and fast liberation and low probability in the meteor trail, respectively. The presence of measurable volatile elements (e.g., Na) in bulk major element analyses and the high degree of oxidation recorded in iron spinel and Ni-rich olivine are evidence for formation in a dense plume and in the deepest oxygen-rich layers of the atmosphere (Cordier et al., 2011; Robin et al., 1992).

Interestingly, BIT-58 represents a large population of airburst spherules (1000s of samples available) and can be considered as covering the full range of potential airburst spherule types at a particular location, due to their sampling as a discrete layer in ice (Harvey et al., 1998) (Fig. 1b). Similarly, the 430 and 480 kyrs airbursts recorded at TAM and WN were also found forming discrete spherule horizons in the EPICA Dome C and Dome Fuji ice cores (Misawa et al., 2010; Narcisi et al., 2007). The TAM and WN airburst spherules were found in glacial sediments sampled on the glacially eroded tops of nunataks, meaning that although these populations may be complete, they cannot be considered as necessarily representative due to dilution in local sediment and/or difficulty in identifying certain spherule types (e.g., SRA spherule were not found among WN spherules but seem to be present in the TAM collection whereas SPA/SPS are absent). The wide range of oxidizing conditions exhibited by particles from the same sampling location is so far unique to WN and BIT-58 particles; from those with iron spinel compositions that are even more reduced than in micrometeorites to those that are extremely oxidized spherules consistent with a formation in the deepest layers of the atmosphere (Gayraud et al., 1996; Toppani and Libourel, 2003). Nucleation of condensate in a plume resulting from a crater forming impact is thought to happen when radial expansion of the hemispherical plume has already started (Glass and Simonson, 2012). Spherules are then deposited over a wide area; possibly worldwide in the case of the largest impacts. Rapid radial expansion during spherule condensation likely results in the geochemical heterogeneity of the plume to be reflected by the geographical distribution of spherules having distinct properties. Conversely, we have shown that BIT-58 and WN spherules before them exhibit a wide range of geochemical properties (e.g., iron spinel composition) at single sampling locations. This can be explained by the upward vertical acceleration of the plume along the rarefied wake left by the passage of the asteroid, resulting in spherules that condensed at various locations in the plume to broadly follow the same trajectory. Subsequently, the mixture of gas and spherules continues to rise owing to its inertia before losing momentum to gravity flattening. The gravitational collapse of the plume result in particles settling over wide areas (Artemieva and Shuvalov, 2010). Here we suggest that the wide redox conditions exhibited by BIT-58 and WN particles are unique to spherules produced by touchdown impacts, i.e., large airbursts, on an icy surface.

The identification of BIT-58 particles as products of airburst provides an important tool to develop a guide to identify these frequent cosmic events in the past. However, airburst events identified so far are limited to Antarctica and we have yet to find occurrences of similar particles in other environments, such as oceanic or continental surfaces. In the case of Tunguska-like airbursts, that is with no direct interaction of the plume with ground material, spherules will be similar to the TAM spherules, that is of limited size (<<100 μm) and highly oxidized due to rapid and intense mixing with atmospheric oxygen (Van Ginneken et al., 2010). In the case of touchdown events, the situation is more complex, as geochemical mixing with terrestrial materials does occur. Obviously, in the case of an impact over Antarctic ice, mixing only between projectile and water vapor occur. Should the impact occur over an ocean, it is likely the range of particle types produced would be similar, if not identical, as the target would equally form water vapor. A similar scenario over a continental surface may produce more complex chemical exchanges. However, due to the limited terrestrial component compared to crater forming events, we can assume that the impactor component will likely be higher than in microtektites and microkrystites for instance, and the plume dense and turbulent enough to result in frequent compound spherules (Glass and Simonson, 2012). Iron spinel is particularly resistant to weathering, as evidenced by the presence in K-Pg microkrystites, therefore finding airburst spherules in diagenetically altered rocks is theoretically possible (Kyte and Smit, 1986).

Currently, small impact craters (<500 m size impactor) on icy surfaces like ice sheets remain undiscovered, leaving the processes behind spherule formation during such impacts largely unknown (Osinski et al., 2022). While it's possible that BIT 58 and WN spherules were formed in such impacts, evidence suggests touchdown scenarios are more likely. As mentioned earlier, the estimated mass of the asteroid responsible for WN spherules implies a large airburst rather than cratering. While such size estimation is challenging for BIT 58 spherules, the characteristics they share with WN particles indicates a similar asteroid size. The presence of euhedral olivine in both WN and BIT 58 spherules suggests slow cooling, distinct from typical cratering-related spherules such as microkrystites. This slow cooling aligns with a longer residence in an airburst plume, indicating a touchdown impact rather than rapid ejection from a plume during cratering event. Van Ginneken et al. (2021) propose a touchdown scenario to explain WN spherule characteristics, but further research is needed to confidently distinguish diagnostic criteria for spherule formation in touchdown impacts versus cratering events.

Not only do BIT-58 particles mark the evidence for the oldest airburst discovered so far, but it confirms the possibility to find evidence of such events in the past. In the long-term, this has important implications for the determination of the frequency of airbursts in the past and, as a consequence, better constrain airburst scenarios for planetary defense. Indeed, a touchdown event would result in total destruction over an area corresponding to the contact between the jet superheated jet and the ground. Should such an event occur over an densely populated area, it would result in millions of casualties and extreme damage over area in the order of 10,000 km^2.

5. Conclusions

Mineralogical and geochemical characteristics of the particles constituting the BIT-58 extraterrestrial dust horizon reveal that these were formed during a large low-latitude airburst between 2.3 and 2.7 million years (Myr) ago. The oxygen isotopic values of the particles exhibit extremely negative $\delta^{18}O$ values, suggesting contamination by Antarctic ice during their formation in the airburst plume. This points to a touchdown impact (or type 2 airburst), when the jet of vaporized impactor maintain momentum and reaches the ground at hypervelocity.

This is the second, and oldest, touchdown impact identified in Antarctica so far. The geochemistry of BIT-58 suggests an ordinary

chondritic impactor, although more analyses are required to draw a definitive conclusion. The deposition at a single site of spherules exhibiting distinct textural groups and varying degrees of oxidation may help distinguish large airburst scenarios from crater forming impacts. This work has important implications for the identification of airburst in the paleorecord.

Declaration of competing interest

The authors declare that they have no known competing financial interests or personal relationships that could have appeared to influence the work reported in this paper.

Acknowledgments

We would like to thank Johan Villeneuve (CRPG) and R. Kanemaru (NIPR) for their assistance during the SIMS and EPMA measurements, respectively. SG acknowledges the support by the Belgian Science Policy (BELSPO) through the BAMM and DESIRED projects. SG also thanks the Research Foundation - Flanders (FWO – Vlaanderen) and the VUB strategic research. RM thanks NIPR International Internship Program for Polar Science 2021 for financial and analytical support. RM acknowledges support from JSPS KAKENHI Grant No. JP23K19080. Frederic Moynier is acknowledged for editorial assistance. We thank two anonymous reviewers for their constructive comments.

Supplementary materials

Supplementary material associated with this article can be found, in the online version, at doi:10.1016/j.epsl.2023.118562.

References

Artemieva, N., Shuvalov, V., 2019. Atmospheric shock waves after impacts of cosmic bodies up to 1000m in diameter. Meteorit. Planet. Sci. 54, 592–608. https://doi.org/10.1111/maps.13229.

Artemieva, N., Shuvalov, V.V., 2010. Tunguska explosion - final remarks. In: Proceedings of the 41st Lunar and Planetary Science Conference, p. 1268.

Artemieva, N.A., Shuvalov, V.V., 2016. From Tunguska to chelyabinsk via Jupiter. Annu. Rev. Earth Planet. Sci. 44, 37–56. https://doi.org/10.1146/annurev-earth-060115-012218.

Boslough, M., 2014. Airburst warning and response. Acta Astronaut. 103, 370–375. https://doi.org/10.1016/j.actaastro.2013.09.007.

Boslough, M., Brown, P., Harris, A., 2015. Updated population and risk assessment for airbursts from near-earth objects (NEOs). In: Proceedings of the 2015 IEEE Aerospace Conference, pp. 1–12. https://doi.org/10.1109/AERO.2015.7119288.

Boslough, M.B.E., Crawford, D.A., 2008. Low-altitude airbursts and the impact threat. Int. J. Impact Eng. 35, 1441–1448. https://doi.org/10.1016/j.ijimpeng.2008.07.053.

Brett, R., Sato, M., 1984. Intrinsic oxygen fugacity measurements on seven chondrites, a pallasite, and a tektite and the redox state of meteorite parent bodies. Geochim. Cosmochim. Acta 48, 111–120. https://doi.org/10.1016/0016-7037(84)90353-3.

Clayton, R.N., Mayeda, T.K., 1999. Oxygen isotope studies of carbonaceous chondrites. Geochim. Cosmochim. Acta 63, 2089–2104. https://doi.org/10.1016/S0016-7037(99)00090-3.

Clayton, R.N., Mayeda, T.K., Goswami, J.N., Olsen, E.J., 1991. Oxygen isotope studies of ordinary chondrites. Geochim. Cosmochim. Acta 55, 2317–2337. https://doi.org/10.1016/0016-7037(91)90107-G.

Cordier, C., Van Ginneken, M., Folco, L., 2011. Nickel abundance in stony cosmic spherules: constraining precursor material and formation mechanisms. Meteorit. Planet. Sci. 46, 1110–1132. https://doi.org/10.1111/j.1945-5100.2011.01218.x.

Ebel, D.S., Grossman, L., 2005. Spinel-bearing spherules condensed from the Chicxulub impact-vapor plume. Geology 33, 293–296. https://doi.org/10.1130/G21136.1.

Folco, L., Cordier, C., 2015. Micrometeorites, in: planetary mineralogy. Eur. Mineral. Union. https://doi.org/10.1180/EMU-notes.15.9.

Folco, L., Rochette, P., Perchiazzi, N., D'Orazio, M., Laurenzi, M.A., Tiepolo, M., 2008. Microtektites from victoria land transantarctic mountains. Geology 36, 291–294. https://doi.org/10.1130/G24528A.1.

Gayraud, J., Robin, E., Rocchia, R., Froget, L., 1996. Formation conditions of oxidized Ni-rich spinel and their relevance to the K/T boundary event. The Cretaceous-Tertiary Event and Other Catastrophes in Earth History. Geological Society of America. https://doi.org/10.1130/0-8137-2307-8.425.

Genge, M.J., Engrand, C., Gounelle, M., Taylor, S., 2008. The classification of micrometeorites. Meteorit. Planet. Sci. 43, 497–515. https://doi.org/10.1111/j.1945-5100.2008.tb00668.x.

Genge, M.J., Grady, M.M., 1999. The fusion crusts of stony meteorites: implications for the atmospheric reprocessing of extraterrestrial materials. Meteorit. Planet. Sci. 34, 341–356. https://doi.org/10.1111/j.1945-5100.1999.tb01344.x.

Gersonde, R., Kyte, F.T., Bleil, U., Diekmann, B., Flores, J.A., Gohl, K., Grahl, G., Hagen, R., Kuhn, G., Sierro, F.J., Völker, D., Abelmann, A., Bostwick, J.A., 1997. Geological record and reconstruction of the late Pliocene impact of the Eltanin asteroid in the Southern Ocean. Nature 390, 357–363. https://doi.org/10.1038/37044.

Glass, B.P., Simonson, B.M., 2012. Distal Impact Ejecta Layers: A Record of Large Impacts in Sedimentary Deposits, Impact Studies. Springer, Berlin Heidelberg.

Glass, B.P., Burns, C.A., 1988. Microkrystites: a new term for impact-produced glassy spherules containing primary crystallites. In: Ryder, G. (Ed.), pp. 455–458.

Grisart, A., Casado, M., Gkinis, V., Vinther, B., Naveau, P., Vrac, M., Laepple, T., Minster, B., Prié, F., Stenni, B., Fourré, E., Steen-Larsen, H.C., Jouzel, J., Werner, M., Pol, K., Masson-Delmotte, V., Hoerhold, M., Popp, T., Landais, A., 2022. Sub-millennial climate variability from high-resolution water isotopes in the EPICA Dome C ice core. Clim. Past 18, 2289–2301. https://doi.org/10.5194/cp-18-2289-2022.

Harvey, R.P., Dunbar, N.W., Esser, R.P., McIntosh, W.C., Nishiizumi, K., Taylor, S., Caffee, M.W., 1998. Meteoritic event recorded in Antarctic ice. Geology 26, 607–610. https://doi.org/10.1130/0091-7613(1998)026<0607:MERIAI>2.3.CO;2.

Kawamura, K., Abe-Ouchi, A., Motoyama, H., Ageta, Y., Aoki, S., Azuma, N., Fujii, Y., Fujita, K., Fujita, S., Fukui, K., Furukawa, T., Furusaki, A., Goto-Azuma, K., Greve, R., Hirabayashi, M., Hondoh, T., Hori, A., Horikawa, S., Horiuchi, K., Igarashi, M., Iizuka, Y., Kameda, T., Kanda, H., Kohno, M., Kuramoto, T., Matsushi, Y., Miyahara, M., Miyake, T., Miyamoto, A., Nagashima, Y., Nakayama, Y., Nakazawa, T., Nakazawa, F., Nishio, F., Obinata, I., Ohgaito, R., Oka, A., Okuno, J., Okuyama, J., Oyabu, I., Parrenin, F., Pattyn, F., Saito, F., Saito, Takashi, Saito, Takeshi, Sakurai, T., Sasa, K., Seddik, H., Shibata, Y., Shinbori, K., Suzuki, K., Suzuki, T., Takahashi, A., Takahashi, K., Takahashi, S., Takata, M., Tanaka, Y., Uemura, R., Watanabe, G., Watanabe, O., Yamasaki, T., Yokoyama, K., Yoshimori, M., Yoshimoto, T., 2017. State dependence of climatic instability over the past 720,000 years from Antarctic ice cores and climate modeling. Sci. Adv. 3 https://doi.org/10.1126/sciadv.1600446.

Kyte, F.T., 2002. Composition of impact melt debris from the Eltanin impact strewn field, Bellingshausen Sea. Deep Sea Res. II Top. Stud. Oceanogr. 49, 1029–1047. https://doi.org/10.1016/S0967-0645(01)00140-0.

Kyte, F.T., Smit, J., 1986. Regional variations in spinel compositions: an important key to the Cretaceous/Tertiary event. Geology 14, 485–487. https://doi.org/10.1130/0091-7613(1986)14<485:RVISCA>2.0.CO;2.

Margolis, S.V., Claeys, P., Kyte, F.T., 1991. Microtektites, microkrystites, and spinels from a late pliocene asteroid impact in the Southern Ocean. Science 251 (1979), 1594–1597. https://doi.org/10.1126/science.251.5001.1594.

Matsuoka, K., Skoglund, A., Roth, G., de Pomereu, J., Griffiths, H., Headland, R., Herried, B., Katsumata, K., Le Brocq, A., Licht, K., Morgan, F., Neff, P.D., Ritz, C., Scheinert, M., Tamura, T., Van de Putte, A., van den Broeke, M., von Deschwanden, A., Deschamps-Berger, C., Van Liefferinge, B., Tronstad, S., Melvær, Y., 2021. Quantarctica, an integrated mapping environment for Antarctica, the Southern Ocean, and sub-Antarctic islands. Environ. Model. Softw. 140, 105015 https://doi.org/10.1016/j.envsoft.2021.105015.

Misawa, K., Kohno, M., Tomiyama, T., Noguchi, T., Nakamura, T., Nagao, K., Mikouchi, T., Nishiizumi, K., 2010. Two extraterrestrial dust horizons found in the Dome Fuji ice core, East Antarctica. Earth Planet. Sci. Lett. 289, 287–297. https://doi.org/10.1016/j.epsl.2009.11.016.

Narcisi, B., Petit, J.R., Engrand, C., 2007. First discovery of meteoritic events in deep Antarctic (EPICA-Dome C) ice cores. Geophys. Res. Lett. 34 https://doi.org/10.1029/2007GL030801.

Newton, J., Franchi, I.A., Pillinger, C.T., 2000. The oxygen-isotopic record in enstatite meteorites. Meteorit. Planet. Sci. 35, 689–698. https://doi.org/10.1111/j.1945-5100.2000.tb01452.x.

Osinski, G.R., Pierazzo, E., Grieve, R., Tornabene, L., 2012. Impact Cratering: Processes and Products. Blackwell Publishing Ltd. https://doi.org/10.1002/9781118447307.ch4.

Osinski, G.R., Grieve, R.A.F., Ferrière, L., Losiak, A., Pickersgill, A.E., Cavosie, A.J., Hibbard, S.M., Hill, P.J.A., Bermudez, J.J., Marion, C.L., Newman, J.D., Simpson, S. L., 2022. Impact Earth: A review of the terrestrial impact record. Earth Sci. Rev. 232, 104112. https://doi.org/10.1016/j.earscirev.2022.104112.

Popova, O.P., Jenniskens, P., Emel\textquoterightyanenko, V., Kartashova, A., Biryukov, E., Khaibrakhmanov, S., Shuvalov, V., Rybnov, Y., Dudorov, A., Grokhovsky, V.I., Badyukov, D.D., Yin, Q.Z., Gural, P.S., Albers, J., Granvik, M., Evers, L.G., Kuiper, J., Kharlamov, V., Solovyov, A., Rusakov, Y.S., Korotkiy, S., Serdyuk, I., Korochantsev, A.V., Larionov, M.Yu., Glazachev, D., Mayer, A.E., Gisler, G., Gladkovsky, S.V., Wimpenny, J., Sanborn, M.E., Yamakawa, A., Verosub, K.L., Rowland, D.J., Roeske, S., Botto, N.W., Friedrich, J.M., Zolensky, M. E., Le, L., Ross, D., Ziegler, K., Nakamura, T., Ahn, I., Lee, J.I., Zhou, Q., Li, X.H., Li, Q.L., Liu, Y., Tang, G.Q., Hiroi, T., Sears, D., Weinstein, I.A., Vokhmintsev, A.S., Ishchenko, A.V., Schmitt-Kopplin, P., Hertkorn, N., Nagao, K., Haba, M.K., Komatsu, M., Mikouchi, T., 2013. Chelyabinsk airburst, damage assessment, meteorite recovery, and characterization. Science 342 (1979), 1069–1073. https://doi.org/10.1126/science.1242642.

Robin, E., Bonté, Ph., Froget, L., Jéhanno, C., Rocchia, R., 1992. Formation of spinels in cosmic objects during atmospheric entry: a clue to the Cretaceous-Tertiary boundary event. Earth Planet. Sci. Lett. 108, 181–190. https://doi.org/10.1016/0012-821X(92)90021-M.

Rubin, A.E., Fegley, B., Brett, R., 1988. Oxidation state in chondrites. In: Kerridge, J.F., Matthews, M.S. (Eds.), Meteorites and the Early Solar System. University of Arizona Press, Tucson, pp. 488–511.

Shuvalov, V.V., Artemieva, N.A., 2002. Numerical modeling of Tunguska-like impacts. Planet. Space Sci. 50, 181–192.

Thiemens, M.H., Jackson, T., Zipf, E.C., Erdman, P.W., van Egmond, C., 1995. Carbon Dioxide and Oxygen Isotope Anomalies in the Mesosphere and Stratosphere. Science 270 (1979), 969–972. https://doi.org/10.1126/science.270.5238.969.

Toppani, A., Libourel, G., 2003. Factors controlling compositions of cosmic spinels: application to atmospheric entry conditions of meteoritic materials. Geochim. Cosmochim. Acta 67, 4621–4638. https://doi.org/10.1016/S0016-7037(03)00383-1.

Van Ginneken, M., Folco, L., Perchiazzi, N., Rochette, P., Bland, P.A., 2010. Meteoritic ablation debris from the Transantarctic Mountains: evidence for a Tunguska-like impact over Antarctica ca. 480ka ago. Earth Planet. Sci. Lett. 293, 104–113. https://doi.org/10.1016/j.epsl.2010.02.028.

van Ginneken, M., Genge, M.J., Folco, L., Harvey, R.P., 2016. The weathering of micrometeorites from the transantarctic mountains. Geochim. Cosmochim. Acta 179, 1–31. https://doi.org/10.1016/j.gca.2015.11.045.

Van Ginneken, M., Goderis, S., Artemieva, N., Debaille, V., Decrée, S., Harvey, R.P., Huwig, K.A., Hecht, L., Yang, S., Kaufmann, F.E.D., Soens, B., Humayun, M., Van Maldeghem, F., Genge, M.J., Claeys, P., 2021. A large meteoritic event over Antarctica ca. 430 ka ago inferred from chondritic spherules from the Sør Rondane Mountains. Sci. Adv. 7, eabc1008. https://doi.org/10.1126/sciadv.abc1008.

Van Ginneken, M., Suavet, C., Cordier, C., Folco, L., Rochette, P., Sonzogni, C., Perchiazzi, N., 2012. Oxygen isotope composition of meteoritic ablation debris from the transantarctic mountains: constraining the parent body and implications for the impact scenario. Meteorit. Planet. Sci. 47, 1738–1747. https://doi.org/10.1111/maps.12011.

Zekollari, H., Goderis, S., Debaille, V., Ginneken, M., van, Gattacceca, J., Timothy, A.J., Lenaerts, J.T.M., Yamaguchi, A., Huybrechts, P., Claeys, P., 2019. Unravelling the high-altitude Nansen blue ice field meteorite trap (East Antarctica) and implications for regional palaeo-conditions. Geochim. Cosmochim. Acta 248, 289–310. https://doi.org/10.1016/j.gca.2018.12.035.